Optimal switching policy for performance enhancement of distributed parameter systems based on event-driven control*

Mu Wen-Ying(穆文英)†, Cui Bao-Tong(崔宝同), Lou Xu-Yang(楼旭阳), and Li Wen(李 纹)

Key Laboratory of Advanced Process Control for Light Industry (Ministry of Education), Jiangnan University, Wuxi 214122, *China*

(Received 7 December 2013; revised manuscript received 8 January 2014; published online 22 May 2014)

This paper aims to improve the performance of a class of distributed parameter systems for the optimal switching of actuators and controllers based on event-driven control. It is assumed that in the available multiple actuators, only one actuator can receive the control signal and be activated over an unfixed time interval, and the other actuators keep dormant. After incorporating a state observer into the event generator, the event-driven control loop and the minimum inter-event time are ultimately bounded. Based on the event-driven state feedback control, the time intervals of unfixed length can be obtained. The optimal switching policy is based on finite horizon linear quadratic optimal control at the beginning of each time subinterval. A simulation example demonstrate the effectiveness of the proposed policy.

Keywords: distributed parameter systems, optimal switching policy, event-driven

PACS: 02.30.Jr, 07.07.Df, 07.05.Dz **DOI:** 10.1088/1674-1056/23/7/070204

1. Introduction

Recently, sensor and actuator networks have been increasingly applied in environment detection, medical care and military fields to provide efficient monitoring and control of the system process.[1–3] Distributed parameter systems (DPS) represent some physical systems.[4,5] The means to reliably and efficiently use sensors and actuators in the processes modeled by DPS have been extensively discussed in Refs. [6]–[11]

Actuator and controller switching has been widely studied for the performance improvement of control systems. In the present study, it is assumed that in the networks with multiple actuators, only one actuator is activated over a given time interval of fixed length and then switched on to a new actuator in the subsequent time interval. Both the actuators and control signals are selected for switching according to the smallest optimal value at the beginning of each time interval of the associated linear quadratic cost-to-go. With the practical advantage in reducing the input energy and cost, the switching policy has been widely discussed in Refs. [12]–[17].

In most of current studies, the switching is periodically triggered by a clock. EI-Farra *et al.*[12] studied the scheduling policy of finding an actuator and controller to improve the control authority and enhance the ability of the system to minimize the effects of disturbances in nonlinear transport-reaction processes. Iftime and Demetriou[13] extended this study to optimal control of switched distributed parameter systems with spatially scheduled actuators. Sha[16] Studied a control pulse combination of pulse train controlled switching converter and its multi-periodicity analysis. Sun[17] proposed the finite-time consensus problem of the leader-following multi-agent system under switching network topologies.

However, the clock-driven switching increases the digital communication among the sensors, actuators and controllers in the control loop has a considerable influence on the overall loop performance. In order to reduce the load of the communication, the event-driven control loop is considered during the switching process determined by events. Once the event is detected, the actuators are switched. The event-driven controlling and communication have been investigated by several researchers.[18–21] Lunze and Lehmann[8] proposed a novel method of event-based state feedback control, in which a control input generator is used to simulate a continuous feedback between two consecutive events. Subsequently, they extend an event-based state feedback approach, which was published recently, towards event-based output feedback[20]. Event-based control aims at reducing the information exchange over the communication network in control systems.[21] Tabuada[22] considered the problem of event-triggered real-time scheduling of stabilizing control tasks. An event-triggering scheme in distributed networked control systems was presented by Wang and Lemmon.[24]

Up to now, the optimal switching of actuator and controller over the time interval trigged by the event-driven control in DPS has seldom been reported. Inspired by these previous works, this paper aims to propose an optimal switching policy of actuators and controllers for performance enhancement of DPS with event-driven control. To attain the above objective, through designing a Luenberger state observer in the

*Project supported by the National Natural Science Foundation of China (Grant Nos. 61174021 and 61104155), the Fundamental Research Funds for the Central Universities, China (Grant Nos. JUDCF13037 and JUSRP51322B), the Programme of Introducing Talents of Discipline to Universities, China (Grant No. B12018), and the Jiangsu Innovation Program for Graduates, China (Grant No. CXZZ13-0740).

†Corresponding author. E-mail: weny815@126.com

© 2014 Chinese Physical Society and IOP Publishing Ltd

event generator and defining the event condition, the switching time interval of unfixed length can be obtained. With the well-established linear quadratic optimal control, multiple actuators are in place when only one actuator is activated over the time interval and the other actuators are dormant. Compared with the performance of the clock-driven switching and non-switching conditions, the performance of the proposed switching algorithm with event-driven control can save energy and extend the lifetime.

The rest of the paper is organized as follows. A few mathematical preliminaries and problem formulation are given in Section 2. Through incorporating a state observer into the event generator, an event-driven state feedback control is presented in Section 3. Section 4 demonstrates the boundedness of the event-driven control loop and minimum inter-event time. The optimal algorithm for the actuator and controller switching of DPS on a finite-time interval is given in Section 5. The simulation example is presented in Section 6. Finally, conclusions are included in Section 7.

2. Problem formulation

Consider the following heat conduction of DPS:

$$\begin{cases} \dfrac{\partial z}{\partial t}(t,x) = \alpha \dfrac{\partial^2 z}{\partial x^2}(t,x) + \sum\limits_{i=1}^{m} b_i(x)u_i(t) + d(x)w(t), \\ z(0,x) \in L^2(\Omega), \\ \dfrac{\partial z}{\partial x}(t,0) = \dfrac{\partial z}{\partial x}(t,l) = 0, \end{cases} \tag{1}$$

$$y(t) = \begin{bmatrix} y_1(t) \\ \vdots \\ y_m(t) \end{bmatrix} = \begin{bmatrix} \int_0^l c_1(x)z(t,x)\mathrm{d}x \\ \vdots \\ \int_0^l c_m(x)z(t,x)\mathrm{d}x \end{bmatrix}, \tag{2}$$

where $z(t,x)$ denotes the state of system (1), $x \in \Omega = [0,l]$ is the spatial coordinate, $t \in [0,\infty]$ is the time variable, $\alpha > 0$. The $b_i(x)$ denotes the spatial distribution of the i-th actuating device, $u_i(t)$ denotes the associated control signal. The $d(x)$ denotes the spatial distribution of the disturbance and $w(t)$ the unknown exogenous input signal (square integrable). The measured signal $y(t)$ denotes the output of the sensing devices, and $c_i(x)$ denotes the spatial distribution of the i-th sensing devices.

Let $\mathcal{X}$ be a Hilbert space with the standard L_2 inner product $\langle\cdot,\cdot\rangle$ and corresponding induced norm $|\cdot|$, $\mathcal{V}$ is a reflexive Banach space with norm denoted by $\|\cdot\|_{\mathcal{V}}$, $\mathcal{V}'$ is the conjugate dual of $\mathcal{V}$, Let $\|\cdot\|^*$ denote the usual norm on $\mathcal{V}'$, we have that[17,18]

$$\mathcal{V} \to \mathcal{X} \to \mathcal{V}', \tag{3}$$

with both embedding being dense and continuous. It is assumed that $|\phi| \le \tau\|\phi\|_{\mathcal{V}}$ for some positive constants.[7] The notation $\langle\cdot,\cdot\rangle$ can also be used to denote the duality paring between $\mathcal{V}$ and $\mathcal{V}'$ induced by the continuous and dense embedding given in Eq. (3).

In order to write the above system in a form that is conductive to the analysis, the original process dynamics Eq. (1) can be represented as an evolution equation, as follows:

$$\begin{aligned} &\dot{z}(t) = Az(t) + Bu(t) + Dw(t), \\ &z_0 \in \mathcal{X}, \end{aligned} \tag{4}$$

where the operator $A : \mathcal{V} \to \mathcal{V}'$ is the infinitesimal generator of a strongly continuous semigroup $T(t)$ on the Hilbert space, which is given by

$$\begin{aligned} &A\phi = \alpha \frac{\mathrm{d}^2\phi}{\mathrm{d}x^2}, \ \ \phi \in \mathcal{V} \text{ with domain,} \\ &\bar{D}(A) = \{\phi \in L_2(0,l) | \phi, \frac{\mathrm{d}\phi}{\mathrm{d}x} \text{ are absolutely continuous,} \\ &\frac{\mathrm{d}^2\phi}{\mathrm{d}x^2} \in L_2(0,l) \text{ and } \frac{\mathrm{d}\phi}{\mathrm{d}x}(0) = \frac{\mathrm{d}\phi}{\mathrm{d}x}(l) = 0\}. \end{aligned}$$

The input operators are parameterized as follows:

$$\langle B_i(x^a)u_i(t), \phi\rangle = \int_0^l b_i(x)\phi(x)u_i(t)\mathrm{d}x, \quad \phi \in \mathcal{V},$$

or in matrix operator form

$$B(x^a)u(t) = [B_1(x^a), \ldots, B_m(x^a)] \begin{bmatrix} u_1(t) \\ \ldots \\ u_m(t) \end{bmatrix}.$$

The disturbance operator D via

$$\langle Dw(t), \phi(x)\rangle = \int_0^l d(x)\phi(x)\mathrm{d}x w(t), \quad \phi \in \mathcal{V}.$$

The output system (2) can be written as

$$y(t) = Cz(t), \tag{5}$$

where the output operator C is parameterized by the sensor locations x^{s}, and the operator is given[2]

$$\begin{aligned} \langle C(x^{\mathrm{s}})\phi, \psi\rangle &= \begin{bmatrix} \langle C_1(x^{\mathrm{s}})\phi, \psi\rangle \\ \vdots \\ \langle C_m(x^{\mathrm{s}})\phi, \psi\rangle \end{bmatrix} \\ &= \begin{bmatrix} \int_0^l c_1(x)\phi(x)\psi(x)\mathrm{d}x \\ \vdots \\ \int_0^l c_m(x)\phi(x)\psi(x)\mathrm{d}x \end{bmatrix}, \quad \phi, \psi \in \mathcal{V}. \end{aligned}$$

We denote the notations $B_i(x^a) = B(x_i^a)$ at actuator location $x_i^a \in \Omega$ and $C_i(x^{\mathrm{s}}) = C(x_i^{\mathrm{s}})$ at sensor location $x_i^{\mathrm{s}} \in \Omega$, where $i = 1, \ldots, m$.

3. Event-driven control

3.1. Continuous state feedback loop

The state-feedback controller is determined by solving the optimization problem of associated linear-quadratic-regulator (LQR) function of the form

$$J(z_0, u) = \langle z(t_f), Mz(t_f)\rangle$$

$$+\int_{t_0}^{t_f}\langle y(s),y(s)\rangle+\langle u(s),Ru(s)\rangle\,\mathrm{d}s \tag{6}$$

on the finite-time interval $[t_0,t_f]$, $t_f<\infty$, where $u(s)$ and $y(s)$ are the input and output trajectories, respectively, and $R\in\mathcal{L}(\mathcal{X})$ is a self-adjoint coercive operator. The control input $u(t)$ which minimizes the cost function J over all trajectories can be represented as $u(t)=-Kz(t)$, with the optimal controller feedback $K=R^{-1}B^*P(t)$, where $P(t)$ is the positive definite solution of the following differential Riccati equation (DRE):

$$\begin{aligned}\frac{\mathrm{d}}{\mathrm{d}t}\langle\phi,P(t)\varphi\rangle &= -\langle\phi,P(t)A\varphi\rangle-\langle A\phi,P(t)\varphi\rangle-\langle C\phi,C\varphi\rangle\\ &\quad+\langle P(t)BR^{-1}B^*P(t)\phi,\varphi\rangle,\\ P(t_f) &= M,\end{aligned} \tag{7}$$

for $\phi,\varphi\in\bar{D}(A)$.

Considering the DPS (Eq. (4)) with the state feedback $u(t)=-Kz(t)$, the continuous closed-loop state feedback system is given as[19]

$$\dot{z}_{CL}(t)=(A-BK)z_{CL}(t)+Dw(t),\quad z_{CL}(0)=z_0, \tag{8}$$

$$y_{CL}(t)=Cz_{CL}(t). \tag{9}$$

Let $\bar{A}=A-BK$. Throughout this paper, we firstly give the following assumptions:

(i) There exists a bounded linear operator F such that $A-FC$ generates an exponentially stable semigroup.

(ii) There exists a bounded linear operator $K=R^{-1}B^*P(t)$ such that $\bar{A}$ generates an exponentially stable semigroup.

(iii) The disturbance $Dw(t)$ is bounded and $w(t)\le w_{max}$.

3.2. Event-driven state feedback

Consider the event-driven control loop is given as the plant system

$$\dot{z}^*(t)=Az^*(t)+Bu^*(t)+Dw(t), \tag{10}$$

$$y^*(t)=Cz^*(t). \tag{11}$$

According to the event-driven control proposed by Lunze and Lehmann,[19] the input generator and the control input generator by the model

$$\begin{cases}\dot{z}_s(t)=\bar{A}z_s(t),\ t\neq t_k,\\ z_s(t_k^+)=z^*(t_k),\ t=t_k,\end{cases} \tag{12}$$

$$y_s(t)=Cz_s(t), \tag{13}$$

$$u^*(t)=-Kz_s(t), \tag{14}$$

for time interval $t\in[t_k,t_{k+1})$ both for the input generator and for the event generator, where $z^*(t)$ is the measured state and $z_s(t)$ is the trajectory of the undisturbed continuous state feedback system for time $t\in[t_k,t_{k+1})$ with initial state $z_s(t_k^+)=z^*(t_k)$. The control input $u^*(t)$ is generated by the undisturbed continuous state feedback system. At each event time t_k, the control input generator receives the current state $z^*(t_k)$ and reinitializes the model (12). The t_k^+ is the instant after the event occurs. Furthermore, an event is generated whenever the relation[20]

$$\|\,z^*(t)-z_s(t)\,\|\ge\bar{e} \tag{15}$$

is satisfied, where $\bar{e}$ is the event threshold.

3.3. Event-driven state feedback based on observer

The above section shows the event generation between the event-driven system $z^*(t)$ and model state system $z_s(t)$. For the state $z^*(t)$ is nonmeasurable upon most occasions. In this case, there is no update of the model state of $z_s(t)$ according to Eq. (12) or event generation according to Eq. (15), therefore, the last scheme should be modified. In this section, a state observer is selected in the event generator and the approximate state $\hat{z}(t)$ is sent to the control input generator at the event time t_k. The structure of the event-driven state feedback control loop based on observer is depicted in Fig. 1.

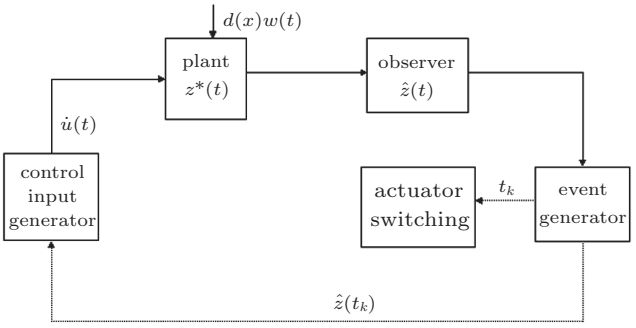


Fig. 1. Event-driven control loop.

The Luenberger observer is designed as

$$\dot{\hat{z}}(t)=A\hat{z}(t)+Bu^*(t)-L(\hat{y}(t)-y^*(t)),\quad \hat{z}(0)=\hat{z}_0, \tag{16}$$

$$\hat{y}(t)=C\hat{z}(t), \tag{17}$$

where $\hat{z}$ is the observer state and L is the observer gain. Notice that due to the presence of interference, we have $z^*(t)\neq\hat{z}(t)$, it is not ensured that the observer state Eqs. (16) and (17) can acquire the state $z^*(t)$ exactly for most of the time.

The control input generator determines the control input $u^*(t)$ in the time interval $t\in[t_k,t_{k+1})$ between two consecutive events based on the information $\hat{z}(t_k)$ received at time t_k. The control input generator is applicable to the model[20]

$$\begin{cases}\dot{\bar{z}}_s(t)=\bar{A}\bar{z}_s(t),\ t\neq t_k,\\ \bar{z}_s(t_k^+)=\hat{z}(t_k),\ t=t_k,\end{cases} \tag{18}$$

$$\bar{y}_s(t)=C\bar{z}_s(t), \tag{19}$$

$$u^*(t)=-K\bar{z}_s(t), \tag{20}$$

of the undisturbed continuous state feedback system. The model state $\bar{z}_s(t)$ is updated with the observer state $\hat{z}(t_k)$ at event time t_k.

A further decisive regulation compared to event-driven state feedback concerns the event generation. An event is triggered when the relation (15) is replaced by the relation[20]

$$\| \hat{z}(t) - \bar{z}_{\rm s}(t) \| \geq \bar{e}_0 \tag{21}$$

is satisfied. At the time $t = 0$, an initial reset yield $\hat{z}(0) = \bar{z}_{\rm s}(0)$. After each reset of the state $\bar{z}_{\rm s}(t_k^+) = \hat{z}(t_k) = \hat{z}(t_k^+)$ holds again, $\|\hat{z}(t_k^+) - \bar{z}_{\rm s}(t_k^+)\| = 0$ is obtained. When the measure state given by

$$\| \hat{z}(t) - \bar{z}_{\rm s}(t) \| < \bar{e}_0 \tag{22}$$

holds, no event occurs.

4. Analysis of the event-driven control loop

4.1. Boundedness analysis

This section shows that the boundedness analysis of the observation error and the boundedness analysis of the event-driven control loop system $z^*(t)$. With the control input (20), the event-driven control loop is given by

$$\dot{z}^*(t) = Az^*(t) - BK\bar{z}_{\rm s}(t) + Dw(t), \quad z(0) = z_0. \tag{23}$$

Assume that the following conditions are satisfied:

(iv) The proper observer gain L is chosen to ensure that $A - LC$ generates an exponentially stable semigroup.

(v) The initial observation error $e(0) \leq e_{0\max}$.

Theorem 1 Consider the DPS in Eqs. (16), (18), and (23) satisfying the above assumptions, then the proposed observation error as well as the difference between the event-driven control loop system $z^*(t)$ and continuous state feedback loop system $z_{\rm CL}(t)$ are bounded. Thus, the state $z^*(t)$ of the event-based control loop is bounded.

Proof According to Eqs. (4) and (16), the observation error between the event-driven control loop state and observer state is described by

$$\dot{e}(t) = (A - LC)e(t) + Dw(t), \tag{24}$$

where $e(t) = z^*(t) - \hat{z}(t)$. An upper bound for the approximation error $e(t)$ can be obtained according to the relation

$$\begin{aligned} \|e(t)\| &= \| \mathrm{e}^{(A-LC)t} e(0) + \| \int_0^t \mathrm{e}^{(A-LC)(t-\tau)} Dw(s)\,\mathrm{d}s \| \\ &\leq \max_{t\in[0,\infty)} \| \mathrm{e}^{(A-LC)t} e_{0\max} \| + \int_0^\infty \| \mathrm{e}^{(A-LC)\tau} \| \,\mathrm{d}\tau \| Dw_{\max} \| \\ &= e_\Delta, \end{aligned} \tag{25}$$

which yields the bounded observation error.

According to Eqs. (22) and (25), an upper bound of difference state $e_{\rm s}(t) = z^*(t) - \bar{z}_{\rm s}(t)$ is obtained from the inequality

$$\begin{aligned} \|e_{\rm s}(t)\| &= \|z^*(t) - \bar{z}_{\rm s}(t)\| \\ &= \|z^*(t) - \hat{z}(t) + \hat{z}(t) - \bar{z}_{\rm s}(t)\| \\ &\leq \|z^*(t) - \hat{z}(t)\| + \|\hat{z}(t) - \bar{z}_{\rm s}(t)\| \\ &\leq e_\Delta + \bar{e}_0, \end{aligned} \tag{26}$$

which implies that the difference state is bounded.

The difference $\bar{e}(t) = z^*(t) - z_{\rm CL}(t)$ between the state $z^*(t)$ of the event-driven control loop and the state $z_{\rm CL}(t)$ of the continuous state feedback loop depends upon the difference state $e_{\rm s}(t)$ introduced in Eqs. (8), (23), and (26), as expressed in the following equations:

$$\begin{aligned} \dot{\bar{e}}(t) &= \dot{z}^*(t) - \dot{z}_{\rm CL}(t) \\ &= Az^*(t) - BK\bar{z}_{\rm s}(t) - (A - BK)z_{\rm CL}(t) \\ &= A\bar{e}(t) - BK\bar{z}_{\rm s}(t) + BKz^*(t) \\ &\quad - BKz^*(t) + BKz_{\rm CL}(t) \\ &= (A - BK)\bar{e}(t) + BK(z^*(t) - \bar{z}_{\rm s}(t)), \\ &= \bar{A}\bar{e}(t) + BKe_{\rm s}(t), \quad \bar{e}(0) = 0. \end{aligned} \tag{27}$$

As $\bar{A}$ generates an exponentially stable semigroup, the state $e_{\rm s}(t)$ is bounded according to Eq. (26). Consequently, the $\bar{e}(t)$ is bounded according to Eq. (27). We know that $z_{\rm CL}(t)$ is bounded under the assumptions (i)–(iii), then the plant state $z^*(t)$ of the event-driven control loop is bounded.

4.2. Minimum inter-event time

Theorem 2 The minimum admissible time internal

$$T_{\min} = \min\{t_{k+1} - t_k | k = 0, 1, 2, \ldots\}$$

that elapses between two consecutive communication event time is bounded.

Proof To obtain the minimum inter-event time, the event condition $\bar{e}_0(t) = \hat{z}(t) - \bar{z}_{\rm s}(t)$ between the observer state and model state is considered, then the difference in the time $[t_k, t_{k+1})$ is given by

$$\begin{aligned} \dot{\bar{e}}_0(t) &= \dot{\hat{z}}(t) - \dot{\bar{z}}_{\rm s}(t) \\ &= A\hat{z}(t) + Bu^*(t) - L(\hat{y}(t) - y^*(t)) - (A - BK)\bar{z}_{\rm s}(t) \\ &= (A - LC)\hat{z}(t) + LCz^*(t) - Az_{\rm s}(t) \\ &= (A - LC)\hat{z}(t) + LC(e_{\rm s}(t) + \bar{z}_{\rm s}(t)) - Az_{\rm s}(t) \\ &= (A - LC)\bar{e}_0(t) + LCe_{\rm s}(t), \end{aligned} \tag{28}$$

with $\bar{e}_0(t_k^+) = 0$, $k = 0, 1, 2, \ldots$

Then, the solution to Eq. (28) is

$$\bar{e}_0(t) = \int_{t_k}^t \mathrm{e}^{(A-LC)(t-\tau)} LCe_{\rm s}(\tau)\,\mathrm{d}\tau.$$

An event should be generated whenever the inequality

$$\left\| \int_{t_k}^t \mathrm{e}^{(A-LC)(t-\tau)} LCe_{\rm s}(\tau)\,\mathrm{d}\tau \right\| \geq \bar{e}_0$$

holds. Moreover, there exists a lower bound time $\tilde{T}$ such that

$$\int_0^{\tilde{T}} \|\mathrm{e}^{(A-LC)\tau}\|\,\mathrm{d}\tau = \frac{\bar{e}_0}{\|LC(e_\Delta+\bar{e}_0)\|}, \tag{29}$$

then we obtain the conclusion that the minimum inter-event time $T_{\min}(T_{\min} \geq \tilde{T})$ is bounded.

5. Optimal switching policy on a finite-time interval

In the above section, we determined the time interval that is triggered by events indicating between two consecutive actuator switchings. In this section, on the basis of event triggering mechanism, an optimal actuator switching policy is realized: one actuator in the available m actuators is activated and the remaining actuators are dormant. The system (4) with m actuators may be written as follows:

$$\dot{z}(t) = Az(t) + [B(x_1^a),\ldots,B(x_m^a)]u(t) + Dw(t), \tag{30}$$

where the vector $u(t)$ has the form $u(t) = [u_1(t),\ldots,u_m(t)]^{\mathrm{T}}$. The individual controller $u_i(t)$, $i = 1,\ldots,m$ is provided for each actuator $B(x_i^a)$. To achieve the switching control setting, the m controllers are designed as[22]

$$u_1(t) = \begin{bmatrix} u_{11}(t) \\ 0 \\ \vdots \\ 0 \end{bmatrix}, \quad u_2(t) = \begin{bmatrix} 0 \\ u_{22}(t) \\ \vdots \\ 0 \end{bmatrix}, \ldots,$$

$$u_m(t) = \begin{bmatrix} 0 \\ 0 \\ \vdots \\ u_{mm}(t) \end{bmatrix}.$$

Hence, when the controller $u_i(t)$ is switched, the i-th actuator is activated. One actuator receives the control input signal $u_i(t)$ in a given time internal, the remaining actuators do not receive any control input signal, that is

$$[B(x_1^a),\ldots,B(x_m^a)]u_i(t) = B(x_i^a)u_{ii}(t). \tag{31}$$

If the duration of a time internal is reached, a new actuator is switched on in the subsequent time internal.

In order to find the optimal actuator switching during a given time instance, the optimal value of the performance index with Eq. (6) of the LQR function over the subinterval $[t_k,t_{k+1})$ is minimized with respect to the m actuator switching. The optimal value $J_{\min}$ is given by

$$J_{\min} = z^{\mathrm{T}}(t_k,x_i^a)P(t_k)z(t_k,x_i^a), \tag{32}$$

where $k = 0,1,2,\ldots,n$, $i = 1,2,\ldots,m$, $P(t)$ solves the parameterized DRE Eq. (7). Based on the DPS Eq. (4), the optimal control law is given by

$$u(t) = -R^{-1}B^*P(t)z(t). \tag{33}$$

Before proceeding with the above considerations, the proposed optimal switching algorithm is summarized as follows.

Algorithm 1 Consider the optimal switching control on a finite-time interval.

Step 1 Make use of the event-driven output feedback control approach to obtain each switching time internal $[t_k,t_{k+1})$, where $k = 0,1,2,\ldots,n$, and $t_0 < t_1 < t_2 < \cdots < t_{n+1} \leq t_{\mathrm{f}}$.

Step 2 At each switching time t_k, $k = 0,1,2,\ldots,n$, form the value of $z^{\mathrm{T}}(t_k,x_i^a)P(t)z(t_k,x_i^a)$, where $P(t)$ is the solution to the DRE (7).

Step 3 Choose the optimal actuator to be activated during the time internal $[t_k,t_{k+1})$ via

$$(x_i^a)^{\mathrm{opt}} = \arg\min_{x_i^a\in\Omega} z^{\mathrm{T}}(t_k)P(t_k)z(t_k).$$

Step 4 If $t_{k+1} < t_{\mathrm{f}}$, repeat step 2 and step 3 for the next time internal $[t_{k+1},t_{k+2})$.

Remark 1 The actuator switching time is triggered by event indication of an intolerable control error. This scheme differs fundamentally from the commonly used clock-driven scheme.

6. Simulation example

The DPS in Eq. (1) is simulated in $\Omega = [0,1]$ with an initial condition $z(0,x) = \sin(\pi x)\,\mathrm{e}^{-7x^2}$. The coefficient is $\alpha = 0.005$. The spatial distribution of the actuator devices with centroid at x_i^a is given by

$$b_i(x) = \begin{cases} \dfrac{1}{\varepsilon}, & x \in [x_i^a-\varepsilon, x_i^a+\varepsilon], \\ 0, & \text{otherwise}. \end{cases}$$

The spatial distribution of the sensing devices with centroid at x_i^{s} is given by

$$c_i(x) = \begin{cases} 1, & x \in [x_i^{\mathrm{s}}-2\varepsilon, x_i^{\mathrm{s}}+2\varepsilon], \\ 0, & \text{otherwise}. \end{cases}$$

The set of the candidate actuator positions are chosen as

$$x_i^a = \frac{(i-0.137)l}{m+1}, \quad i = 1,\ldots,m.$$

The sensor positions and the actuator positions are collocated in the network; that is, $x_i^{\mathrm{s}} = x_i^a$. The disturbance $d(t,x) = 10^{-4}[3\cos(9\pi t/t_{\mathrm{f}}) + 5]\{H[0.2\cos(9\pi t/t_{\mathrm{f}}+0.7) - \varepsilon] - H[0.2\cos(9\pi t/t_{\mathrm{f}}+0.7)+\varepsilon]\}$, where $\varepsilon = 0.05$.

We consider $m = 5$ actuators for switching in the time internal [0 s,9 s], and the LQR parameters are chosen as $M = I$, $R = I$. The observer parameter is $L = 0.1$. It is assumed that the initial condition is satisfied

$$z^*(0,x) = z(0,x) = \cos(\pi x)\,\mathrm{e}^{-7x^2} \neq \hat{z}(0,x)$$

$$= \bar{z}_s(0,x) = \sin(\pi x)\, e^{-7x^2}.$$

In order to obtain the switching time internal more intuitively, we consider the situation when $x = 0.5$. The event threshold is set to be $\bar{e}_0 = 0.05$, and the event condition is $\| \hat{z}(t,0.5) - \bar{z}_s(t,0.5) \| = 0.05$.

From Fig. 2 we note that after the initializing event at time $t_0 = 0$, five further events occur, respectively, in $t_1 = 1.6$ s, $t_2 = 2.48$ s, $t_3 = 3.72$ s, $t_4 = 5.45$ s, and $t_5 = 7.12$ s. According to the switching algorithm, the associated actuator activation optimal sequence is presented in Fig. 3. In this case, we can see that the actuators $B(x_3^a)$ and $B(x_4^a)$ are used most of the time.

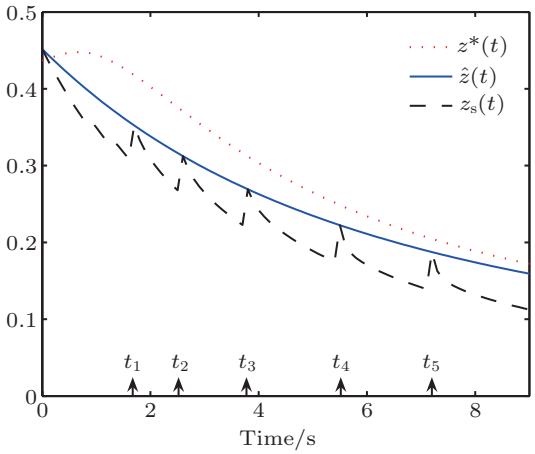


Fig. 2. (color online) Event-driven output feedback control.

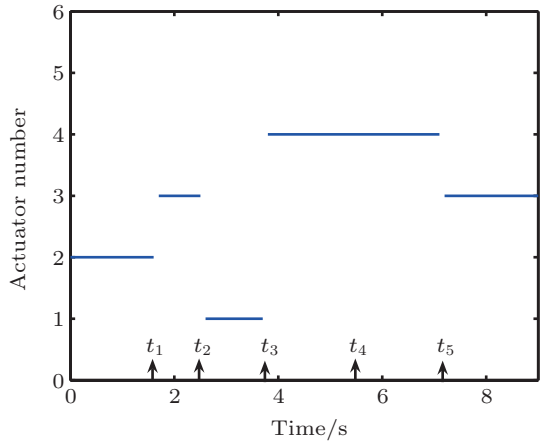


Fig. 3. (color online) Actuator switching sequence based on the event-driven control.

To compare the proposed algorithm with clock-driven switching algorithm, which divide the interval $[0,9]$ into $\Delta t = (t_f - t_0)/6 = 1.5$ s. At the beginning of each time interval $[t_k, t_k + \Delta t)(k = 0,1,2,\ldots,5)$, the smallest value of the optimal cost $z^T(t_k)P(t_k)z(t_k)$ are chosen. The optimal actuator switching allocation is presented in Fig. 4.

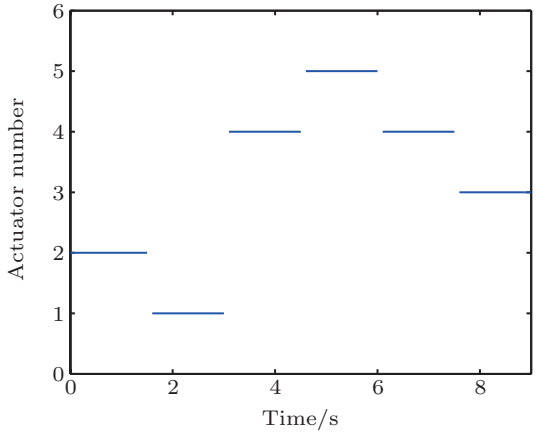


Fig. 4. (color online) Actuator switching sequence based on the clock-driven control.

The optimal cost $J_{\min}(t_k,u)$ on the cumulative L_2 norm defined by $\|z(t,x)\|_{2,2}^2 = \int_0^t \int_0^l z^2(t,x)\,dx\,dt$. Figure 5 shows the evolution of the L_2 state norm for three cases of event-driven switching, clock-driven switching, and non-switching (using actuator $B(x_3^a)$). Compared with the cases of the clock-driven switching and non-switching, the event-driven switching showed an overwhelmingly encouraging performance improvement.

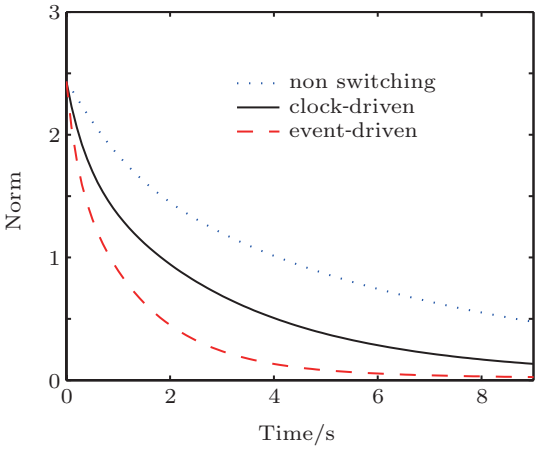


Fig. 5. (color online) Evolution of state L_2 norm.

7. Conclusions

This paper has proposed an optimal switching algorithm of a class of DPS. With the LQR optimal control on finite-time interval, an actuator-plus-controller switching policy has been developed on the basis of the event-driven control. Since the state is not measurable, a state observer is considered in the event generator. By using the event-driven state feedback control based on the Luenberger state observer, a set of different time intervals are available. Both the actuator and controller signals are switched at the beginning of the time intervals. Numerical simulation results have revealed that the performance enhancement can be achieved with the proposed optimal switching policy.

References

[1] Qi H, Wang F B and Deng H 2013 *Acta Phys. Sin.* **62** 104301 (in Chinese)

[2] Zhang C, Fei S M and Zhou X P 2012 *Chin. Phys. B* **21** 120101

[3] Tan F and Huang X H 2013 *Chin. Phys. Lett.* **30** 050701

[4] Li Q, Zhang B H, Cui L G, Fan Z and Athanasios V V 2012 *Chin. Phys. B* **21** 050205

[5] Li W H 2013 *Chin. Phys. B* **22** 016102

[6] He Z R, Wu T L, Qi O Y and Tu Y H 2012 *Chin. Phys. B* **21** 098701

[7] Demetriou M A 2010 *IEEE Trans. Autom. Control* **55** 1570

[8] Demetriou M A 2008 *Proceedings of the* 47*th IEEE Conference on Decision and Control*, December 9–11, 2008, Worcester, USA, p. 215

[9] Demetriou M A 2010 *Automatica* **46** 300

[10] Demetriou M A and Kazantzis N 2005 *Comput. Chem. Eng.* **29** 867

[11] Armaou A and Demetriou M A 2006 *Chem. Eng. Sci.* **61** 7351

[12] El-Farra N H, Demetriou M A and Christofides P D 2008 *Chem. Eng. Sci.* **63** 3537

[13] Iftime O V and Demetriou M A 2009 *Automatica* **45** 312

[14] Iftime O V and Demetriou M A 2007 *Proceedings of the* 46*th IEEE Conference on Decision and Control*, December 12–17, 2007, New Orleans, USA, p. 206

[15] Demetriou M A and Kazantzis N 2004 *Automatica* **40** 415

[16] Sha J and Xu J P 2013 *Acta Phys. Sin.* **62** 218402 (in Chinese)

[17] Sun F L and Zhu W 2013 *Chin. Phys. B* **22** 110204

[18] Cairano S D, Bemporad A and Júlvez J 2009 *Automatica* **45** 1243

[19] Lunze J and Lehmann D 2010 *Automatica* **46** 211

[20] Lehmann D and Lunze J 2011 *Proceedings of the* 19*th Mediterranean conference on Control and Automation*, June 20–23, 2011, Corfu, Greece, p. 982

[21] Lehmann D and Lunze J 2011 *Proceedings of the* 18*th IFAC World Congress*, August 28–September 2, 2011, Milano, Italy, p. 3262

[22] Tabuada P 2007 *IEEE Trans. Autom. Control* **52** 1680

[23] Stöcker C and Lunze J 2013 *J. Appl. Math. Mech.* **21** 525

[24] Wang X F, Lemmon M D and Lyu M R 2011 *IEEE Trans. Autom. Control* **56** 586

[25] Lions J L and Magenes E 1972 *Non-Homogeneous Boundary Value Problems* (I) (New York: Springer-Verlag) pp. 23–25

[26] Tanabe H 1979 *Equations of Evolution* (London: Pitman) pp. 19–21